# TCPILP: Tangential Cutting Plane Enabled Iterative Linear Programming for Loss Minimization in AC-DC Radial Distribution Network

Giriwar Chaurasia, Ajay Singh, Puspendu Ghosh, Subho Paul, *MIEEE*, and Narayana Prasad Padhy, *SMIEEE*

***Abstract*—Large penetration of DC energy resources, like solar PV panels and DC power electronic loads, causes the emergence of merging DC power network and the existing AC network by voltage source converters (VSCs). These new-generation AC-DC distribution networks (DNs) are complex in architecture and hard to model analytically for their management. The past literature either suggested the second-order cone programming (SOCP) based relaxation or the first-order Taylor series based linearization, followed by an iterative algorithm to simplify and solve the non-convex quadratic constraints associated with the line power flow and VSC. However, SOCP relaxed methods suffer from scalability issues, and the Taylor series-based simplification sometimes derives an infeasible solution. In this regard, this paper first formulated a non-convex AC-DC radial DNs (RDNs) loss minimization framework, followed by proposing an iterative linear programming algorithm where the infeasibility caused by the Taylor series approximation is rectified by incorporating the linear Tangential cutting plane inequality constraints into the optimization portfolio and adding the penalty variable minimization with the objective function. The superiority of the proposed strategy over existing methods are established by simulating on the 33 and 132-bus AC-DC RDN test systems.**

***Index Terms*—AC-DC radial distribution network (RDN), iterative linear programming (ILP), tangential cutting plane (TCP), Taylor series expansion, voltage source converter (VSC)**

## I. Introduction

The recent focus on renewable energy resources, especially solar photovoltaic (PV) panels, and the recent development in various DC power electronics loads like electric vehicles, LED lights, DC computers, etc, have led to the integration of DC networks with the existing AC electrical RDNs to avoid the utilization of a large number of AC-DC converters, and that inherently reduce power conversion losses. This merger of the AC and the DC networks using VSCs results the new age distribution network architecture, named as AC-DC RDN.

In recent years, several research works have been conducted to explore the viability of AC-DC RDN by developing an optimal planning framework [1], the optimal configuration of the network topology [2], and power flow algorithms [3]. The optimal power flow (OPF) portfolios are generally framed as non-convex programming (NCP) and traditionally often suggested to solve using heuristic search techniques like the Genetic algorithm (GA) [4], Evolutionary algorithm [5], NSGA-II [6], etc. To avoid the complexity associated with the solution process for NCP frameworks, a few studies, [7]–[10], adopted second-order cone (SOC) relaxation for solving the NCP OPF, energy management, optimal coordination of the VSCs, and resilience enhancement problems, respectively. Reference [11] co-optimized the operation of VSCs and the charging of electric buses in an AC-DC RDN by solving a mixed-integer SOCP (MISOCP) framework. Previously, the authors also adopted SOCP for formulating a distributed loss minimization algorithm in [12]. Tong et al. [13] developed an over-voltage averse OPF problem as quadratic-convex model. Another MISOCP-based method is proposed in [14] to optimize the operation of the VAR compensation devices and inverters. To further simplify the solution process, [15]–[17] adopted auxiliary variables, piecewise linearization, polyhedral linearization, etc., to convert the NCP problem to a simple LP. However, the existing studies suffer from following flaws:

1) The heuristic techniques [4]–[6] are able to deal with the original NCP frameworks. However, they fails to ensure the stability and convergence of the derived solution.
2) The SOCP adopted methods, [7]–[14], guarantee convergence but require longer solution time for large systems.
3) The LP based models [15]–[17] are fast converging but linear approximations introduce error and that deviate outcomes from the global optimality.

To overcome these, in [18], the authors proposed a sequential MILP (s-MILP) algorithm by employing first-order Taylor series linearization for the quadratic expressions. But the method did initialization by solving the original NCP and lacks an infeasibility correcting mechanism, resulting longer solution time and more iterations. This paper further improves the ILP algorithm by introducing the TCP constraints for infeasibility handling. The new method, named as TCP Enabled Iterative LP (TCPILP), does median value initialization and shows fast convergence. The specific contributions are listed below:

1) A non-convex loss minimization problem is formulated for AC-DC RDN and then simplified by adopting suitable linearization techniques. However, to handle the possible infeasibilities related to AC-DC power flow and VSC operations, TCP constraints are introduced and added as inequality with the linear optimization framework. The TCP ensures the feasibility in the successive iterations by limiting the search space at the boundary of the original non-convex problem by incorporating penalty parameters in the inequality constraints.
2) The objective function is revised to minimize the penalty variable along with the network loss and then the framework is solved iteratively till the convergence criteria is met i.e., zero valued penalty variable and no change in the objective function. Median based initialization reduces the computation burden and solution time.

G. Chaurasia, A. Singh, P. Ghosh and S. Paul are with the AMRIT Research Lab, Department of Electrical Engineering, Indian Institute of Technology (BHU), Varanasi, UP, India. N. P. Padhy is with the Department of Electrical Engineering, Indian Institute of Technology Roorkee, UK, India (Email: (giriwarchaurasia.rs.eee24, subho.eee)@itbhu.ac.in, nppadhy@ee.iitr.ac.in).
This research work is supported by ANRF, India sponsored DAMSON project (File number: ANRF/ECRG/2024/000987/ENS), (Project ID: R&D/ANRF/4211/EE/25-26/680) (Awarded to S. Paul)

979-8-3315-8138-1

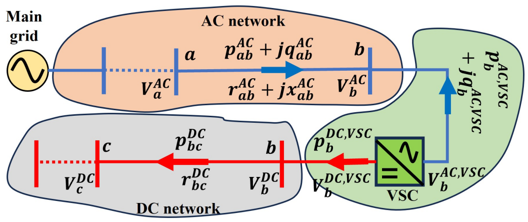


Fig. 1. Schematic of a typical AC-DC RDN

3) The simulation study on 33- and 132-bus AC-DC RDN proves the performance supremacy of the proposed TCPILP against SOCP, LP, and s-MILP based methods.

## II. Loss Minimization Problem for AC-DC RDN

Here, the AC-DC RDN is modeled as a connected graph, consisting of three parts (shown in Fig. 1), viz. the AC/DC networks having AC/DC buses and lines, and the VSCs, which are installed to perform AC to DC conversion and vice-versa. The analytical notations are described in Table I. Solar PV panels are installed at different locations in the network and associated with the smart inverters if it is at the AC network. The optimization portfolio is formulated to regulate the reactive power dispatch from the PV inverters and VSCs to minimize the active power loss ($P_{loss}^{T}$) for the RDN [12].

$$\begin{aligned} Min \quad P_{loss}^{T} = \sum_{a\in M_{AC}} \sum_{b\in M_{AC}} l_{ab}^{AC} r_{ab}^{AC} + \\ \sum_{a\in M_{DC}} \sum_{b\in M_{DC}} l_{ab}^{DC} r_{ab}^{DC} + \sum_{b\in M} p_{b,loss}^{VSC} \end{aligned} \tag{1}$$

$$\text{s.t., } p_{b,L}^{AC} - p_b^{PV} = \sum_{a:a\to b} \left(p_{ab}^{AC} - l_{ab}^{AC} r_{ab}^{AC}\right) - \sum_{c:b\to c} \left(p_{bc}^{AC}\right) \tag{2}$$

$$q_{b,L}^{AC} - q_b^{PV} = \sum_{a:a\to b} \left(q_{ab}^{AC} - l_{ab}^{AC} x_{ab}^{AC}\right) - \sum_{c:b\to c} \left(q_{bc}^{AC}\right) \tag{3}$$

$$\begin{aligned} v_b^{AC} = v_a^{AC} - 2\left(r_{ab}^{AC} p_{ab}^{AC} + x_{ab}^{AC} q_{ab}^{AC}\right) + \\ \left(\left(r_{ab}^{AC}\right)^2 + \left(x_{ab}^{AC}\right)^2\right) l_{ab}^{AC}, \forall a, b \in M_{AC} \end{aligned} \tag{4}$$

$$\left(p_{ab}^{AC}\right)^2 + \left(q_{ab}^{AC}\right)^2 = v_a^{AC} l_{ab}^{AC} \tag{5}$$

$$-\sqrt{\left(s_b^{PV}\right)^2 - \left(p_b^{PV}\right)^2} \le q_b^{PV} \le \sqrt{\left(s_b^{PV}\right)^2 - \left(p_b^{PV}\right)^2} \tag{6}$$

$$\left(V_{min}^{AC}\right)^2 \le v_a^{AC}, v_b^{AC} \le \left(V_{max}^{AC}\right)^2, \forall a, b \in M_{AC} \tag{7}$$

$$p_{b,L}^{DC} - p_b^{PV} = \sum_{a:a\to b} \left(p_{ab}^{DC} - l_{ab}^{DC} r_{ab}^{DC}\right) - \sum_{c:b\to c} \left(p_{bc}^{DC}\right) \tag{8}$$

$$v_b^{DC} = v_a^{DC} - 2\left(r_{ab}^{DC} p_{ab}^{DC}\right) + \left(r_{ab}^{DC}\right)^2 l_{ab}^{DC}, \forall a, b \in M_{DC} \tag{9}$$

$$\left(p_{ab}^{DC}\right)^2 = v_a^{DC} l_{ab}^{DC} \tag{10}$$

$$\left(V_{min}^{DC}\right)^2 \le v_a^{DC}, v_b^{DC} \le \left(V_{max}^{DC}\right)^2, \forall a, b \in M_{DC} \tag{11}$$

$$0.9 \le \xi_b^{VSC} \le 1.0 \tag{12}$$

$$p_b^{AC,VSC} = \beta_{VSC} p_b^{DC,VSC} \tag{13}$$

$$\left(p_b^{AC,VSC}\right)^2 + \left(q_b^{AC,VSC}\right)^2 = \left(p_{b,loss}^{VSC}/\alpha_{VSC}\right)^2 \tag{14}$$

$$p_b^{AC,VSC} + p_b^{DC,VSC} + p_{b,loss}^{VSC} = 0 \tag{15}$$

TABLE I
Nomenclature for the AC-DC RDN modelling

| Symbol | Description |
|---|---|
| $M$ | Total number of buses in AC–DC RDN (index: $a$, $b$, $c$) |
| $M_{AC/DC}$ | Total number of buses in AC/DC network |
| $V_b^{AC/DC}$ | Voltage magnitude of AC/DC bus $b$ (pu) |
| $I_{ab}^{AC/DC}$ | Current magnitude flowing between buses $a$ and $b$ (pu) |
| $p_{ab}^{AC/DC}$ | Active power flow between buses $a$ and $b$ (pu) |
| $q_{ab}^{AC}$ | Reactive power flow between buses $a$ and $b$ (pu) |
| $r_{ab}^{AC/DC}$ | AC/DC network line resistance (pu) |
| $x_{ab}^{AC}$ | AC network line reactance (pu) |
| $p_b^{PV}/q_b^{PV}$ | Active/reactive power dispatch from PV inverter (pu) |
| $s_b^{PV}$ | PV inverter apparent power rating at bus $a$ (pu) |
| $V_b^{AC/DC,VSC}$ | Voltage magnitude at AC/DC side of the VSC (pu) |
| $p_b^{AC/DC,VSC}$ | Active power at AC/DC side of VSC (pu) |
| $q_b^{AC,VSC}$ | Reactive power at AC side of VSC (pu) |
| $s_b^{VSC}$ | Apparent power rating of VSC at bus $b$ (pu) |
| $\alpha_{VSC}$ | VSC loss coefficient |
| $\beta_{VSC}$ | VSC efficiency |
| $\xi_b^{VSC}$ | Amplitude-modulation index for VSC |
| $p_{b,loss}^{VSC}$ | Active-power loss at VSC (pu) |
| $p_{b,L}^{AC/DC}$ | Active-power demand at AC/DC bus $a$ (pu) |
| $q_{b,L}^{AC}$ | Reactive-power demand at AC bus $a$ (pu) |
| $V_{min}^{AC/DC}$ | Minimum allowable voltage limit at AC/DC bus (pu) |
| $V_{max}^{AC/DC}$ | Maximum allowable voltage limit at AC/DC bus (pu) |

$$V_b^{AC,VSC} = 0.612 \xi_b^{VSC} V_b^{DC,VSC} \tag{16}$$

$$\left(p_b^{AC,VSC}\right)^2 + \left(q_b^{AC,VSC}\right)^2 \le \left(s_b^{VSC}\right)^2 \tag{17}$$

Here, $l_{ab}^{AC/DC} = \left(I_{ab}^{AC/DC}\right)^2$, $v_b^{AC/DC} = \left(V_b^{AC/DC}\right)^2$

The objective function (1) is the summation of AC network (1st term), DC network (2nd term) losses, and power loss at VSC (3rd term). Equations (2)-(5) represent the branch flow model (BFM) for the AC network, denoting nodal active and reactive power balance, node voltage, and apparent line power flow, respectively [12]. The reactive power dispatch from the PV inverters at the AC network is limited by the inequality (6). The AC bus voltage magnitude follows the boundary limit (7). The DC network BFM is provided in (8)-(10), denoting active power balance, bus voltage, and line flows, respectively. DC bus voltage is bounded by (11). The operation of VSC is modeled by the constraints (12)-(17), representing the range of modulation index, relation between AC and DC sides active power, active power loss, active power balance, relation between AC and DC sides voltage magnitude, boundary limit on apparent power dispatch at AC side, respectively.

## III. Solution Approach

### A. Linearization Techniques

The problem described in Section II is an NCP due to the presence of bi-linear terms in constraint (16), quadratic equality (5), (10), and (14), and quadratic inequality (17). These non-convexity need to be linearized for fast convergence.

979-8-3315-8138-1

*1) McCormick Envelopes:* Equality constraint (16) is non-convex due to bi-linear term $\xi_b^{VSC} V_b^{DC,VSC}$, where $V_b^{DC,VSC}$ in pu corresponding to DC network base voltage. McCormick envelopes are employed to linearize the bi-linear term using auxiliary variable $\Omega$ [19]. The linear inequalities (19)-(22) are added to the problem and (16) is replaced with (18). Envelopes possess exactness if the optimal decisions i.e. $\Omega^*, \xi_b^{VSC*}$, and $V_b^{DC,VSC*}$ satisfies $\Omega^* = \xi_b^{VSC*} V_b^{DC,VSC*}$. It is reported in [20] that the exactness can be obtained if the continuous variables are of short range. Generally, the variation range of the per unit voltage magnitude is 0.2 pu (0.9 pu to 1.1 pu), and variation range of $\xi_b^{VSC}$ is only 0.1 (0.9 to 1.0). So, it is worth telling that the envelopes are tight.

$$V_b^{AC,VSC} = 0.612\Omega, \quad \Omega = \xi_b^{VSC} V_b^{DC,VSC} \tag{18}$$

$$\Omega \leq \left(\xi_b^{VSC} V_{min}^{DC} + 1.0 V_b^{DC,VSC} - 1.0 V_{min}^{DC}\right) \tag{19}$$

$$\Omega \leq \left(\xi_b^{VSC} V_{max}^{DC} + 0.9 V_b^{DC,VSC} - 0.9 V_{max}^{DC}\right) \tag{20}$$

$$\Omega \geq \left(\xi_b^{VSC} V_{min}^{DC} + 0.9 V_b^{DC,VSC} - 0.9 V_{min}^{DC}\right) \tag{21}$$

$$\Omega \geq \left(\xi_b^{VSC} V_{max}^{DC} + 1.0 V_b^{DC,VSC} - 1.0 V_{max}^{DC}\right) \tag{22}$$

*2) First Order Taylor Series:* Each quadratic term in the constraints (5), (10), (14), and (17), are approximated by their first order Taylor series by neglecting the higher order terms. The Taylor series evaluation point at iteration $i$ is denoted by the hat ($\hat{x}$) variables. The linear constraints are [18]:

$$\begin{aligned} &2p_{ab}^{AC}\left(\hat{p}_{ab}^{AC}\right)^i + 2q_{ab}^{AC}\left(\hat{q}_{ab}^{AC}\right)^i - \left(\left(\hat{p}_{ab}^{AC}\right)^i\right)^2 \\ &- \left(\left(\hat{q}_{ab}^{AC}\right)^i\right)^2 = v_a^{AC}\left(\hat{l}_{ab}^{AC}\right)^i + l_{ab}^{AC}\left(\hat{v}_a^{AC}\right)^i \end{aligned} \tag{23}$$

$$2p_{ab}^{DC}\left(\hat{p}_{ab}^{DC}\right)^i = v_a^{DC}\left(\hat{l}_{ab}^{DC}\right)^i + l_{ab}^{DC}\left(\hat{v}_a^{DC}\right)^i \tag{24}$$

$$\begin{aligned} &2p_b^{AC,VSC}\left(\hat{p}_b^{AC,VSC}\right)^i + 2q_b^{AC,VSC}\left(\hat{q}_b^{AC,VSC}\right)^i \\ &- \left(\left(\hat{p}_b^{AC,VSC}\right)^i\right)^2 - \left(\left(\hat{q}_b^{AC,VSC}\right)^i\right)^2 \\ &= \frac{1}{\alpha_{VSC}^2}\left(2p_{b,loss}^{VSC}\left(p_{b,loss}^{VSC}\right)^i - \left(\left(\hat{p}_{b,loss}^{VSC}\right)^i\right)^2\right) \end{aligned} \tag{25}$$

$$\begin{aligned} &2p_b^{AC,VSC}\left(\hat{p}_b^{AC,VSC}\right)^i + 2q_b^{AC,VSC}\left(\hat{q}_b^{AC,VSC}\right)^2 \\ &- \left(\left(\hat{p}_b^{AC,VSC}\right)^i\right)^2 - \left(\left(\hat{q}_b^{AC,VSC}\right)^i\right)^2 \leq \left(s_b^{VSC}\right)^2 \end{aligned} \tag{26}$$

Therefore, the linearized loss minimization problem is [18] :

**L1:** Min. (1), s.t. (2)-(4), (6)-(9), (11)-(13), (15), (18)-(26).

## B. Infeasibility Handling with Tangential Cutting Plane

In Section III-A2, the quadratic terms are linearized by first-order Taylor series while neglecting the second and other higher-order terms. Hence, there is a possibility that the solution point derived at iteration $i$ may not follow the actual quadratic constraint and show the following conditions:

$$\left(\hat{p}_{ab}^{AC}\right)^2 + \left(\hat{q}_{ab}^{AC}\right)^2 \neq \hat{v}_a^{AC}\hat{l}_{ab}^{AC} \tag{27}$$

$$\left(\hat{p}_{ab}^{DC}\right)^2 \neq \hat{v}_a^{DC}\hat{l}_{ab}^{DC} \tag{28}$$

$$\left(\hat{p}_b^{AC,VSC}\right)^2 + \left(\hat{q}_b^{AC,VSC}\right)^2 \neq \left(\hat{p}_{b,loss}^{VSC}/\alpha_{VSC}\right)^2 \tag{29}$$

$$\left(p_b^{AC,VSC}\right)^2 + \left(q_b^{AC,VSC}\right)^2 > \left(s_b^{VSC}\right)^2 \tag{30}$$

Now, the following conditions, (31)-(33), can be observed for the infeasibility (27)-(30).

$$\text{Either } \left(\hat{p}_{ab}^{AC}\right)^2 + \left(\hat{q}_{ab}^{AC}\right)^2 < \hat{v}_a^{AC}\hat{l}_{ab}^{AC}, \text{ or } > \hat{v}_a^{AC}\hat{l}_{ab}^{AC} \tag{31}$$

$$\text{Either } \left(\hat{p}_{ab}^{DC}\right)^2 < \hat{v}_a^{DC}\hat{l}_{ab}^{DC}, \text{ or } > \hat{v}_a^{DC}\hat{l}_{ab}^{DC} \tag{32}$$

$$\begin{aligned} &\text{Either } \left(\hat{p}_b^{AC,VSC}\right)^2 + \left(\hat{q}_b^{AC,VSC}\right)^2 \\ &< \left(\hat{p}_{b,loss}^{VSC}/\alpha_{VSC}\right)^2, \text{ or } > \left(\hat{p}_{b,loss}^{VSC}/\alpha_{VSC}\right)^2 \end{aligned} \tag{33}$$

Hence, to shift the solution point from infeasible search space to the feasible region, TCP constraints (34)-(40) are introduced with penalty variables $\mu_{b/ab,vio}^{AC/DC/VSC,+/-} \geq 0$. Constraint (34) is added to avoid the VSC dispatch infeasibility (30).

$$\begin{aligned} p_b^{AC,VSC}\left(\hat{p}_b^{AC,VSC}\right)^i + q_b^{AC,VSC}\left(\hat{q}_b^{AC,VSC}\right)^i \\ \leq \left(s_b^{VSC}\right)^2 + \mu_{b,vio}^{VSC} \end{aligned} \tag{34}$$

The infeasibility (31) is managed by introducing two linear tangential cutting plane inequality constraints as given below,

$$p_{ab}^{AC}\left(\hat{p}_{ab}^{AC}\right)^i + q_{ab}^{AC}\left(\hat{q}_{ab}^{AC}\right)^i \leq v_a^{AC}\hat{l}_{ab}^{AC} + l_{ab}^{AC}\hat{v}_a^{AC} + \mu_{ab,vio}^{AC,+} \tag{35}$$

$$v_a^{AC}\hat{l}_{ab}^{AC} + l_{ab}^{AC}\hat{v}_a^{AC} \leq p_{ab}^{AC}\left(\hat{p}_{ab}^{AC}\right)^i + q_{ab}^{AC}\left(\hat{q}_{ab}^{AC}\right)^i + \mu_{ab,vio}^{AC,-} \tag{36}$$

***Proposition 1:*** *If at any iteration $i$, the derived solutions give $\mu_{ab,vio}^{AC,+} = \mu_{ab,vio}^{AC,-} = 0$ after satisfying the constraints (35) and (36), and the solution does not alter between two consecutive iterations, i.e., $i-1$ and $i$, then*

$$\left(\left(\hat{p}_{ab}^{AC}\right)^i\right)^2 + \left(\left(\hat{q}_{ab}^{AC}\right)^i\right)^2 = \left(\hat{v}_a^{AC}\right)^i\left(\hat{l}_{ab}^{AC}\right)^i$$

Similar way, the infeasibility (32) and (33) can be avoided by adding the following inequalties into optimization framework

$$p_{ab}^{DC}\left(\hat{p}_{ab}^{DC}\right)^i \leq v_a^{DC}\hat{l}_{ab}^{DC} + l_{ab}^{DC}\hat{v}_a^{DC} + \mu_{ab,vio}^{DC,+} \tag{37}$$

$$v_a^{DC}\hat{l}_{ab}^{DC} + l_{ab}^{DC}\hat{v}_a^{DC} \leq p_{ab}^{DC}\left(\hat{p}_{ab}^{AC}\right)^i + \mu_{ab,vio}^{DC,-} \tag{38}$$

$$\begin{aligned} p_b^{AC,VSC}\left(\hat{p}_b^{AC,VSC}\right)^i + q_b^{AC,VSC}\left(\hat{q}_b^{AC,VSC}\right)^i \\ \leq \left(1/\alpha_{VSC}^2\right)p_{b,loss}^{VSC}\left(\hat{p}_{b,loss}^{VSC}\right)^i + \mu_{b,vio}^{VSC,+} \end{aligned} \tag{39}$$

$$\begin{aligned} \frac{1}{\alpha_{VSC}^2}p_{b,loss}^{VSC}\left(\hat{p}_{b,loss}^{VSC}\right)^i \leq p_b^{AC,VSC}\left(\hat{p}_b^{AC,VSC}\right)^i \\ + q_b^{AC,VSC}\left(\hat{q}_b^{AC,VSC}\right)^i + \mu_{b,vio}^{VSC,-} \end{aligned} \tag{40}$$

As per the "Proposition 1", the AC-DC OPF feasible solutions are only obtained by making the penalty variables zero. Hence,

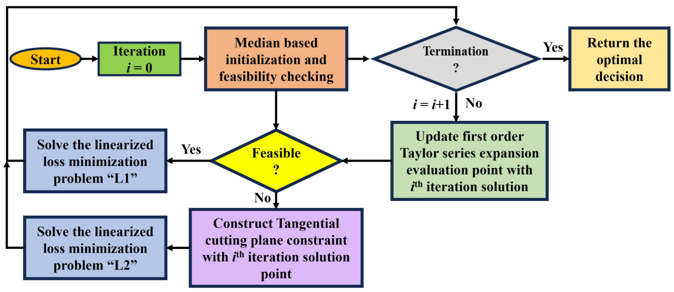


Fig. 2. Flow chart of the proposed TCPILP algorithm

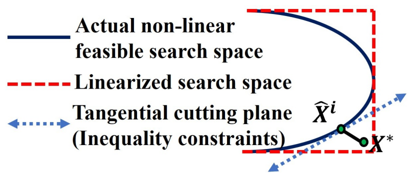


Fig. 3. Philosophy of tangential cutting plane constraint for feasibility

the objective function is revised by adding the penalty variable minimization with the loss minimization, as shown.

$$\textbf{L2:}\ Min \quad P_{loss}^{T} + \sum_{b\in M}\left(\mu_{b,vio}^{VSC} + \mu_{b,vio}^{VSC,+} + \mu_{b,vio}^{VSC,-}\right) + \sum_{a\in M}\sum_{b\in M}\left(\mu_{ab,vio}^{AC,+} + \mu_{ab,vio}^{AC,-} + \mu_{ab,vio}^{DC,+} + \mu_{ab,vio}^{DC,-}\right)$$

S.t. (2)-(4), (6)-(9), (11)-(13), (15), (18)-(26), and (34)-(40).

### C. Proposed TCPILP Algorithm

The proposed tangential cutting plane enabled iterative linear programming approach, abbreviated as TCPILP, is depicted in Fig. 2. At the beginning (i.e., when iteration count $i = 0$), the initial solution point for the first-order Taylor series expansion is estimated using the median values of the decision variables within their permissible ranges. The feasibility of this initial point is then verified by computing the corresponding AC-DC power flows and VSC dispatches. If it violates the feasibility, it will be adjusted to lie within the feasible operating region. After proper initialization, the LP-based loss minimization problem is solved iteratively. After completion of every iteration, the termination condition is verified. The algorithm is set to terminate when following three conditions are satisfied simultaneously. First, the penalty parameter values are zero, which denotes feasibility; second, the difference between the obtained objective function values of two consecutive iterations are lesser than the threshold limit (i.e., 1e-5), and third, the mismatch for the McCormick envelopes are lesser than 0.001 pu to ensure exactness [14]. If any of these conditions are not met, then the iteration counter is updated and the Taylor series evaluation point is updated using the most recent solution.

After updating the Taylor series evaluation point, the feasibility of the new solution point is re-investigated. If it does not satisfy either VSC or AC-DC power flow or both constraints, the TCP constraints are constructed and added with the "L1" problem to form the "L2" problem. As shown in Fig. 3, the TCP ensures feasibility in the successive iterations by updating the infeasible solution $X^*$ at iteration $i$ to the feasible solution

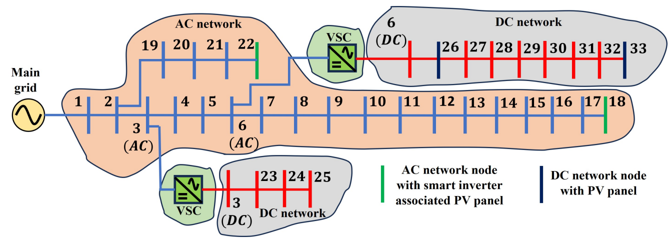


Fig. 4. Schematic of 33-bus AC-DC RDN with PV panels

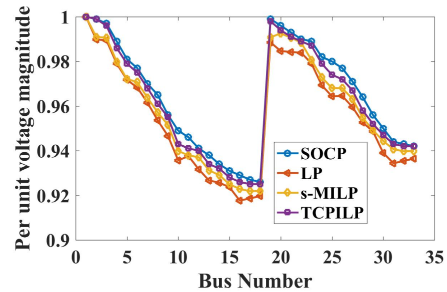


Fig. 5. 33-bus system node voltages for LP, SOCP, s-MILP, and TCPILP

$\hat{X}^i$. The TCILP algorithm ensures convergence to the global optima (i.e., the KKT-optimal point) when the iterative process terminates with all penalty variables reduced to zero.

## IV. Simulation Study

The efficacy of the TCPILP algorithm is validated on 33-bus AC-DC RDN consisting of one AC network, 2 DC networks and 2 VSCs [18] (Fig. 4). The system has 4 PVs of 500 kW rating (2 at AC network and 2 at DC network). The AC network PV panels are associated with 600 kVA inverters. Base load condition with 1 pu solar power generation and 1 pu substation voltage is considered for simulation scenario. The efficiency and power factor of VSCs are 0.95. The bus voltages are allowed to vary between 0.9 pu and 1.1 pu corresponding to their base values. The simulation is carried out on an i7 computer with 16 GB RAM, and the "linprog" solver in MATLAB is used to solve the L1 and L2 problems.

The performance comparison is done between TCPILP and other methods viz. SOCP [7]–[13], LP [17], and s-MILP [18]. The LP method is formulated by adopting piecewise linearization for simplifying the quadratic terms. The solution obtained from the SOCP-based method is considered as the reference to validate the optimality of other methods. The simulation results are provided in Fig. 5 and Table II. It is noted that all methods achieve near optimal solution (see the voltage profile at Fig. 5). However, LP possesses the highest optimality gap because of the approximation taken in piecewise linearization, but produces the result in the least time. The s-MILP reduces the optimality gap, but the initialization process takes a longer time. Further, to avoid the effect of the initialization with an infeasible solution point, it completes more iterations (almost 15 sec per iteration). Now, the proposed TCPILP shows a good trade-off between accuracy and solution time. It shows the least optimality gap with solution time lower than SOCP and s-MILP based methods. Compared to s-MILP, TCPILP needs fewer iterations because of its inherent capability to manage the infeasibility with TCPs in subsequent iterations. Again, unlike s-MILP, median-based initialization reduces the

979-8-3315-8138-1

TABLE II

SIMULATION RESULTS FOR 33-BUS AC-DC TEST SYSTEM

| Parameters | SOCP [7]–[13] | LP [17] | s-MILP [18] | TCPILP |
|---|---|---|---|---|
| Optimal $P_{loss}^T$ (kW) | 89.36 | 92.67 | 91.14 | 90.02 |
| Optimality gap (%) | Base | 3.70 | 1.99 | 0.74 |
| Total iteration needed | - | - | 7 | 4 |
| Initialization time (min) | - | - | 3.5 | 0.11 |
| Solution time (min) | 1.75 | 0.88 | 5.25 | 1.36 |

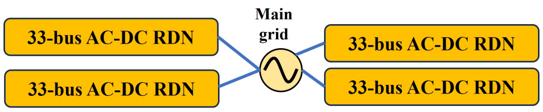


Fig. 6. Schematic of 132-bus AC-DC RDN

solution time significantly. Further, the McCormick mismatch is around 0.0005 pu, which reflects its tightness.

The performance of TCPILP for a large network is validated on 132-bus AC-DC RDN (Fig. 6), adopted from [18]. The simulation results are summarized in Table III. It is noted that with the increase in network size, the optimality gap increases for LP, but it is still the fastest solution process. SOCP method also experiences a significant increase in solution time. Both s-MILP and TCPILP complete more iterations before termination (compared to 33-bus case), but large initialization time makes s-MILP the worst-performing, as it needs to solve a large number of non-convex constraints. Comparing with the existing methods, it is noted that the TCPILP method outperforms LP and s-MILP in terms of optimality gap, and SOCP and s-MILP in terms of solution time. The McCormick envelopes are exact for 132-bus test systems as well (gap is around 0.0008 pu). This makes it suitable for real-life applications in bulk networks.

## V. CONCLUSION

This article proposes a new tangential cutting plane enabled iterative linear programming algorithm to solve the loss minimization optimization problem of AC-DC RDN. First, the method linearizes the non-linear terms using the McCormick envelopes and the first-order Taylor series. Later, to correct the infeasible evaluation point at the Taylor series at the successive iterations, tangential cutting plane constraints with penalty parameters are introduced as inequality constraints. The minimization of the penalty parameters makes the solutions AC-DC power flow and VSC operation feasible. The simulation study on 33-bus and 132-bus test systems show the suitability of the proposed method in terms of optimality gap and solution time compared with the existing state-of-the-art techniques. In the future, the authors would like to expand the work to develop a multi-period multi-objective OPF problem with energy storage and electric vehicle. The present algorithm will be updated by incorporating temporal and spatial decomposition methods for reducing computation complexity and convergence time.

TABLE III

SIMULATION RESULTS FOR 132-BUS AC-DC TEST SYSTEM

| Parameters | SOCP [7]–[13] | LP [17] | s-MILP [18] | TCPILP |
|---|---|---|---|---|
| Optimal $P_{loss}^T$ (kW) | 336.25 | 357.49 | 344.58 | 339.48 |
| Optimality gap (%) | Base | 6.31 | 2.48 | 0.96 |
| Total iteration needed | - | - | 12 | 5 |
| Initialization time (min) | - | - | 16.34 | 0.23 |
| Solution time (min) | 15.73 | 2.47 | 36.14 | 3.73 |

## REFERENCES


[1] H. Farias de Barros, M.-C. Alvarez-Herault, B. Raison, and Q. T. Tran, "Optimal ac/dc distribution systems expansion planning from dso's perspective considering topological constraints," *IEEE Trans. Power Del.*, vol. 38, no. 5, pp. 3417–3428, 2023.

[2] L. Zhang et al., "Optimal configuration of hybrid ac/dc distribution network considering the temporal power flow complementarity on lines," *IEEE Trans. Smart Grid*, vol. 13, no. 5, pp. 3857–3866, 2022.

[3] K. Murari, N. P. Padhy, and S. Kamalasadan, "A backward-forward sweep based power flow algorithm for generalized ac-dc distribution network with distributed generations," *IEEE Trans. Ind. Appl.*, vol. 59, no. 4, pp. 5032–5047, 2023.

[4] A. A. Eajal et al., "Stochastic centralized dispatch scheme for ac/dc hybrid smart distribution systems," *IEEE Trans. Sustain. Energy*, vol. 7, no. 3, pp. 1046–1059, 2016.

[5] F. Qiao and J. Ma, "Voltage/var control for hybrid distribution networks using decomposition-based multiobjective evolutionary algorithm," *IEEE Access*, vol. 8, pp. 12 015–12 025, 2020.

[6] L. Shang et al., "Multiobjective optimization for hybrid ac/dc distribution network structure considering reliability," in *2021 IEEE Sustain. Power Energy Conf. (iSPEC)*, 2021, pp. 3034–3041.

[7] M. M.-U.-T. Chowdhury, K. Murari, M. S. Hasan, and S. Kamalasadan, "Optimal power flow (opf) analysis for ac–dc active distribution networks utilizing second-order cone programming (socp) approach," *IEEE Trans. Ind. Inform.*, vol. 21, no. 5, pp. 3555–3564, 2025.

[8] Y. Fu, Z. Zhang, Z. Li, and Y. Mi, "Energy management for hybrid ac/dc distribution system with microgrid clusters using non-cooperative game theory and robust optimization," *IEEE Trans. Smart Grid*, vol. 11, no. 2, pp. 1510–1525, 2020.

[9] F. Sun, J. Ma, M. Yu, and W. Wei, "A robust optimal coordinated droop control method for multiple vscs in ac–dc distribution network," *IEEE Trans. Power Systems*, vol. 34, no. 6, pp. 5002–5011, 2019.

[10] L. Zhang et al., "A coordinated restoration method of hybrid ac/dc distribution network for resilience enhancement," *IEEE Trans. Smart Grid*, vol. 14, no. 1, pp. 112–125, 2023.

[11] Y. Zhang et al., "Co-optimizing electric tourist buses and vsc to enhance the flexibility of hybrid ac/dc distribution networks with distributed pv," *IEEE Transactions on Smart Grid*, vol. 16, no. 1, pp. 741–753, 2025.

[12] S. Paul et al., "Predictor-corrector accelerated admm method for the socp-relaxed ac-dc optimal power flow," in *2024 IEEE Power Energy Soc. Gen. Meeting (PESGM)*, 2024, pp. 1–5.

[13] B. Tong et al., "An overvoltage-averse model for renewable-rich ac/dc distribution networks considering the sensitivity of voltage violation probability," *IEEE Trans. Sustain. Energy*, vol. 16, no. 1, pp. 613–626, 2025.

[14] Q. Sun et al., "Network-side carbon emission reduction via dispatching power electronic devices in ac–dc hybrid distribution systems," *IEEE Trans. Autom. Sc. Eng.*, vol. 22, pp. 20 406–20 419, 2025.

[15] S. Paul and N. P. Padhy, "Impact assessment of real time demand control on active ac/dc hybrid distribution networks," in *2020 IEEE Power Energy Soc. Gen. Meeting (PESGM)*, 2020, pp. 1–5.

[16] M. Dabbaghjamanesh et al., "Sensitivity analysis of renewable energy integration on stochastic energy management of automated reconfigurable hybrid ac–dc microgrid considering dlr security constraint," *IEEE Trans. Ind. Inform.*, vol. 16, no. 1, pp. 120–131, 2020.

[17] H. M. A. Ahmed and M. M. A. Salama, "Energy management of ac–dc hybrid distribution systems considering network reconfiguration," *IEEE Trans. Power Syst.*, vol. 34, no. 6, pp. 4583–4594, 2019.

[18] S. Paul, A. Sharma, and N. P. Padhy, "Risk constrained energy efficient optimal operation of a converter governed ac/dc hybrid distribution network with distributed energy resources and volt-var controlling devices," *IEEE Trans. Ind. Appl.*, vol. 57, no. 4, pp. 4263–4277, 2021.

[19] G. P. McCormick, "Computability of global solutions to factorable nonconvex programs: Part-i—convex underestimating problems," *Math. Program.*, vol. 10, no. 1, pp. 147–175, 1976.

[20] S. R. Shukla, S. Paudyal, and M. R. Almassalkhi, "Efficient distribution system optimal power flow with discrete control of load tap changers," *IEEE Trans. Power Syst*, vol. 34, no. 4, pp. 2970–2979, 2019.


979-8-3315-8138-1